Supplemental data

Super-enhancers reorganization controls re-sensitization of oxaliplatin-resistant FBXW7-mutated colorectal cancer

Vanessa Tolotto[1#], Nicolò Gualandi[1#], Monica Colitti[2], Raffaella Picco[1], Ylenia Cortolezzis[1], Francesca D'Este[1], Mariachiara Gani[1], Wayne W. Hancock[3], Giovanni Terrosu[4], Cristina Degrassi[5], Claudio Brancolini[6], Luigi Xodo[1], Eros Di Giorgio[1*]

Running title: Epigenetic treatment of FBXW7 mutated colorectal cancer

[1]Laboratory of Biochemistry, Department of Medicine, Università degli Studi di Udine, p.le Kolbe 4, 33100 Udine, Italy

[2]Dipartimento di Scienze agroalimentari, ambientali e animali, Università degli Studi di Udine, Udine, Italy

[3]Division of Transplant Immunology, Department of Pathology and Laboratory Medicine, Children's Hospital of Philadelphia and Perelman School of Medicine, University of Pennsylvania, Philadelphia, Pennsylvania, USA

[4]Department of Medicine, Università degli Studi di Udine, Institute for Biomedicine, P.le Kolbe 4, Udine 33100, Italy

[5]MTTLab, Via Gallina 5 - 34122 Trieste - Italy

[6]Laboratory of Epigenomics, Department of Medicine, Università degli Studi di Udine, p.le Kolbe 4, 33100 Udine, Italy

Co-first authorship

Correspondence: eros.digiorgio@uniud.it

Lead contact: eros.digiorgio@uniud.it

Supplementary Tables

Supplementary Table 1. Protein expression levels (z-score) of HDAC4, HDAC5 and 365 E3 ligases available for the indicated 375 cancer cell lines of the Cancer Cell Line Encyclopedia.

Supplementary Table 2. Characteristics of CRC patients whose biopsies were used for the TMA.

Supplementary Table 3. .bed files of the SEs identified in HCT-116 cells:
CRC1: WT Untreated esiCT
CRC2: WT Untreated esiCT + OxPt
CRC3: WT Untreated esiHDAC4
CRC4: WT Untreated esiHDAC4 + OxPt
CRC5: *FBXW7*$^{-/-}$ Untreated esiCT
CRC6: *FBXW7*$^{-/-}$ Untreated esiCT + OxPt
CRC7: *FBXW7*$^{-/-}$ Untreated esiHDAC4
CRC8: *FBXW7*$^{-/-}$ Untreated esiHDAC4 + OxPt

Supplementary Table 4. .bed files of the SEs belonging to cluster 2 and 3.

Supplementary Table 5. minimal signature of 51 genes associated to cluster 2 and 3.

Supplementary Table 6. TCGA sample ID of CRC patients bearing FBXW7 LOF.

Supplementary Table 7. .bed files of the SEs belonging to refined cluster 2 and 3.

Supplementary Table 8. Expression levels of genes associated to refined cluster 2 and 3 of SEs in GSE28691.

Supplementary Table 9. Expression levels of genes associated to refined cluster 2 and 3 of SEs in GSE72970.

Supplementary Table 10. Minimal signatures of 9 and 37 genes associated to refined cluster 3 and 2 which displayed prognostic value.

Supplementary Table 11. List and sequences of primers used for this study.

Supplementary Figures

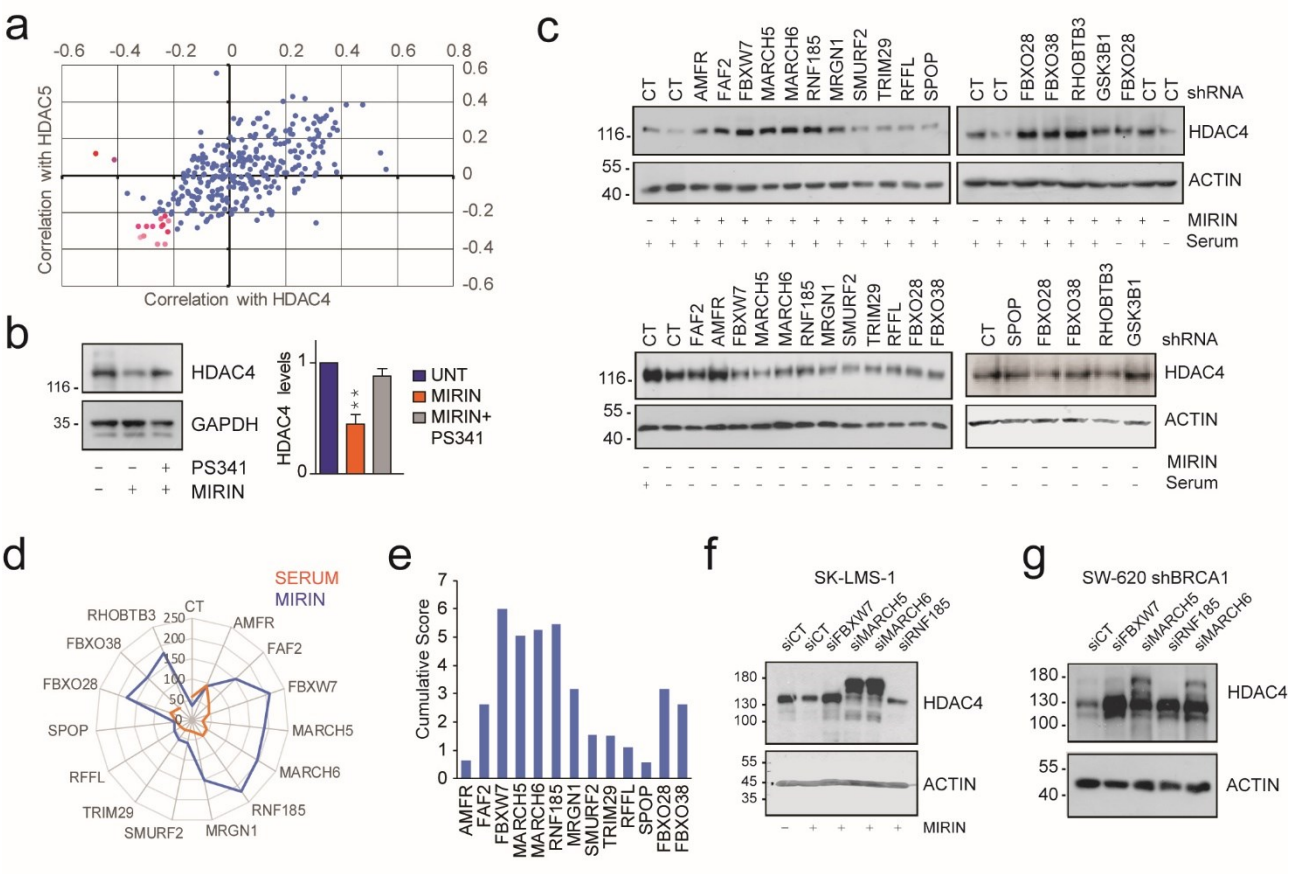

Supplementary Figure 1. Identification of the E3 ligases involved in HDAC4 degradation through *in silico* and *in vitro* screenings. a. *In silico* screening representing the correlation between HDAC4 and HDAC5 (the two most expressed class IIa HDACs) and 365 E3 ligases available for the indicated 375 cancer cell lines of the Cancer Cell Line Encyclopedia. 14 E3 ligases highlighted in pink were selected for being negatively correlated with HDAC4 and/or HDAC5 protein levels**. b.** Immunoblot analysis and quantification of HDAC4 protein levels in 293T cells treated with Mirin 20µM for 36h and PS341 1µM for the last 8h. **c.** Secondary screening: the expression of the 14 identified E3 ligases was knocked-down with lentiviral shRNAs in 293T cells. Silenced cells were treated with Mirin 20µM for 24h or cultivated in serum starvation conditions (0,2% FBS, 24h), then cells were harvested and the levels of HDAC4 were assessed by immunoblotting. **d.** Radar chart reporting the percentual of residual HDAC4 after Mirin treatment or serum starvation and the knock-down of the reported 14 E3-ligases in respect to shCT. **e.** Cumulative score expressed the ratio between HDAC4 protein levels in Mirin vs Serum starvation. **f,g**. Tertiary screening: Immunoblot analysis of HDAC4 in SK-LMS-1 cells silenced for the indicated E3-ligases and treated for 36h with Mirin (f) or in SW620 cells (g) knocked-down for BRCA1 and in which the expression of the indicated E3-ligases was silenced for 48h.

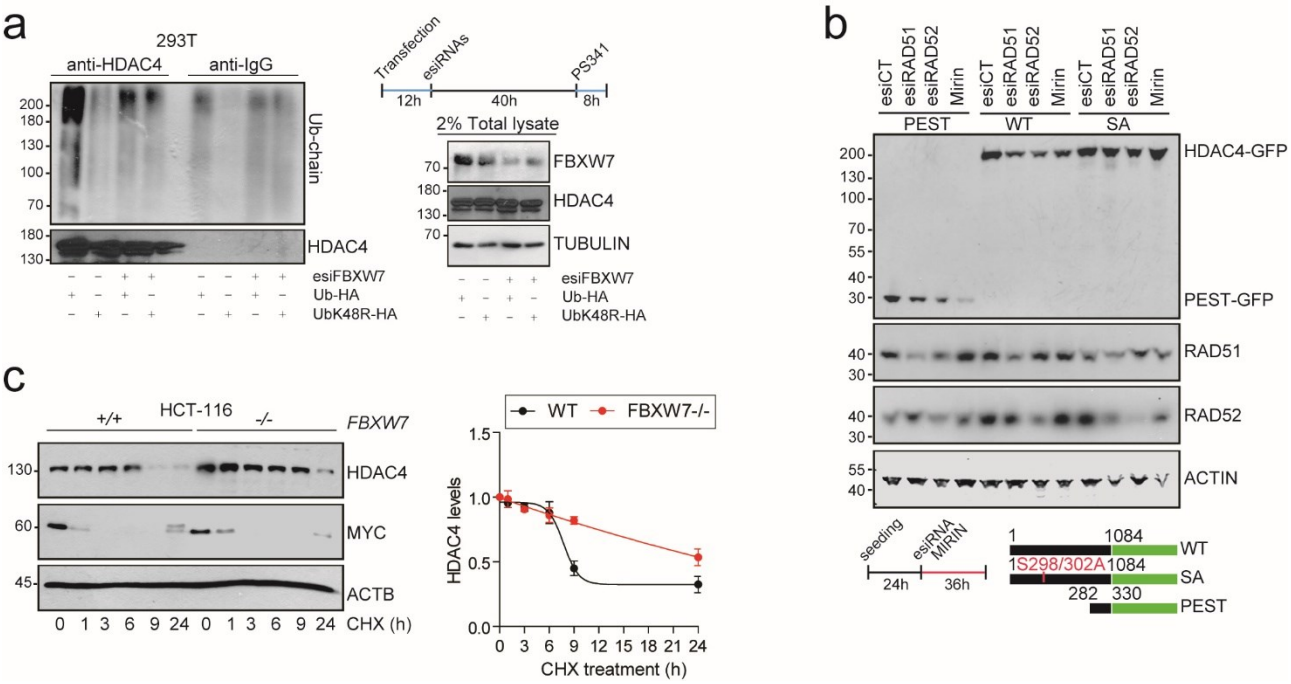

Supplementary Figure 2. FBXW7 controls HDAC4 K48 poly-ubiquitylation by binding to its N-terminal domain. a. Poly-ubiquitylation assay on HDAC4 immunopurified from 293T cells transfected with Ub-HA or UbK48R-HA and silenced or not for FBXW7, as indicated. Anti-FBXW7 was used to check silencing efficacy in 2% total lysate used as input. **b.** Immunoblot analysis of the indicated protein in 293T cells expressing PEST-GFP, HDAC4 WT-GFP or the phospho-dead HDAC4 S298A-GFP, silenced for RAD51 or RAD52 or treated with Mirin 20μM as indicated. The scheme illustrates the HDAC4 mutants used. PEST domain (aminoacids 282-330) is the minimal domain of HDAC4 responding to HR blockage. **c.** Immunoblot analysis and evaluation of HDAC4 and MYC protein stability in HCT-116 WT or *FBXW7*$^{-/-}$ cells through the time after the treatment with cycloheximide 10 μg/ml.

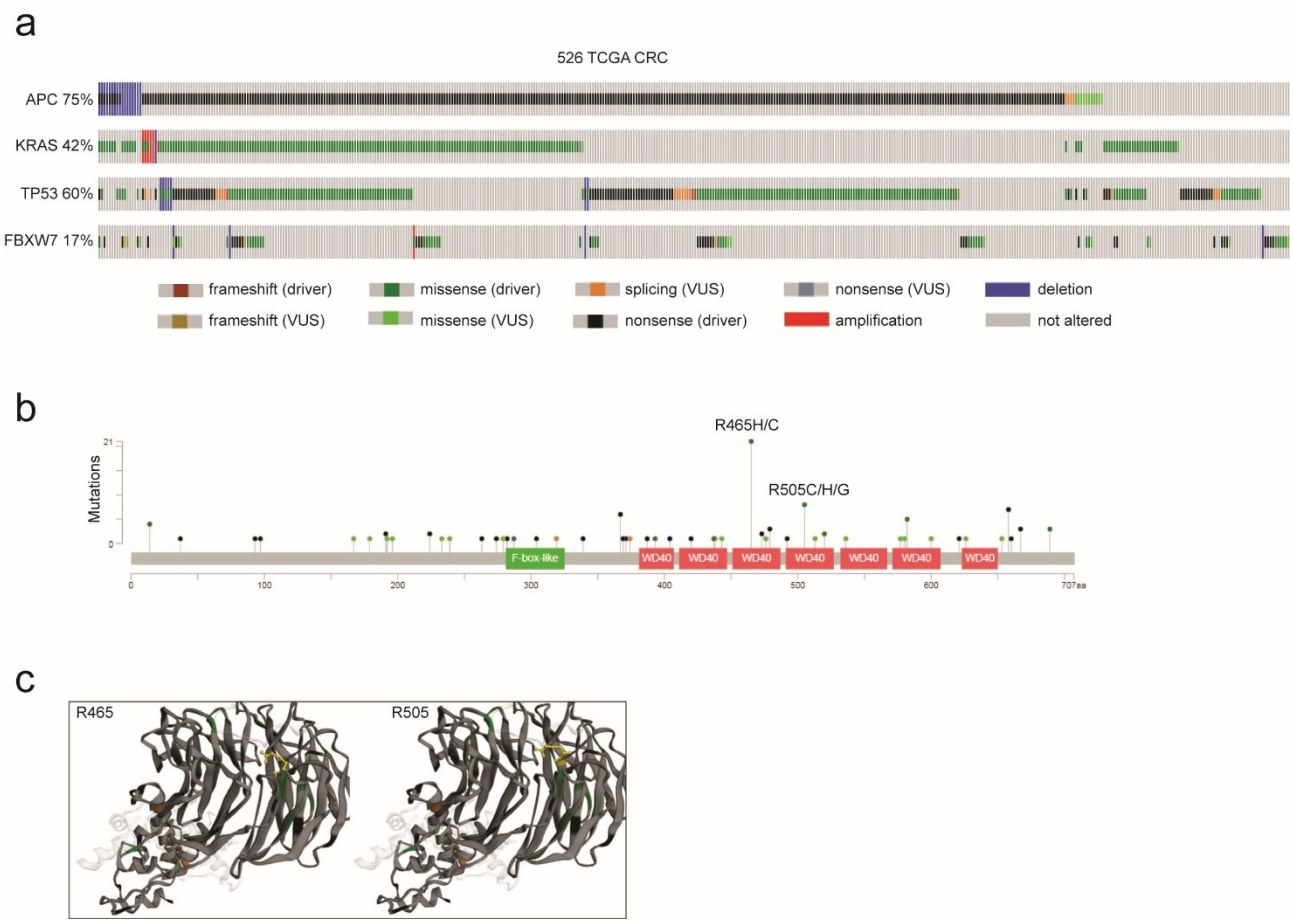

Supplementary Figure 3. Frequency and impact of FBXW7 LOF mutations in CRC. a. Oncoprint diagram of mutational profile of 526 TCGA CRC samples. **b.** FBXW7 Hot-spot mutations in TCGA CRC samples. **c.** R465 and R505 are highlighted in yellow in the 3D structure of FBXW7.

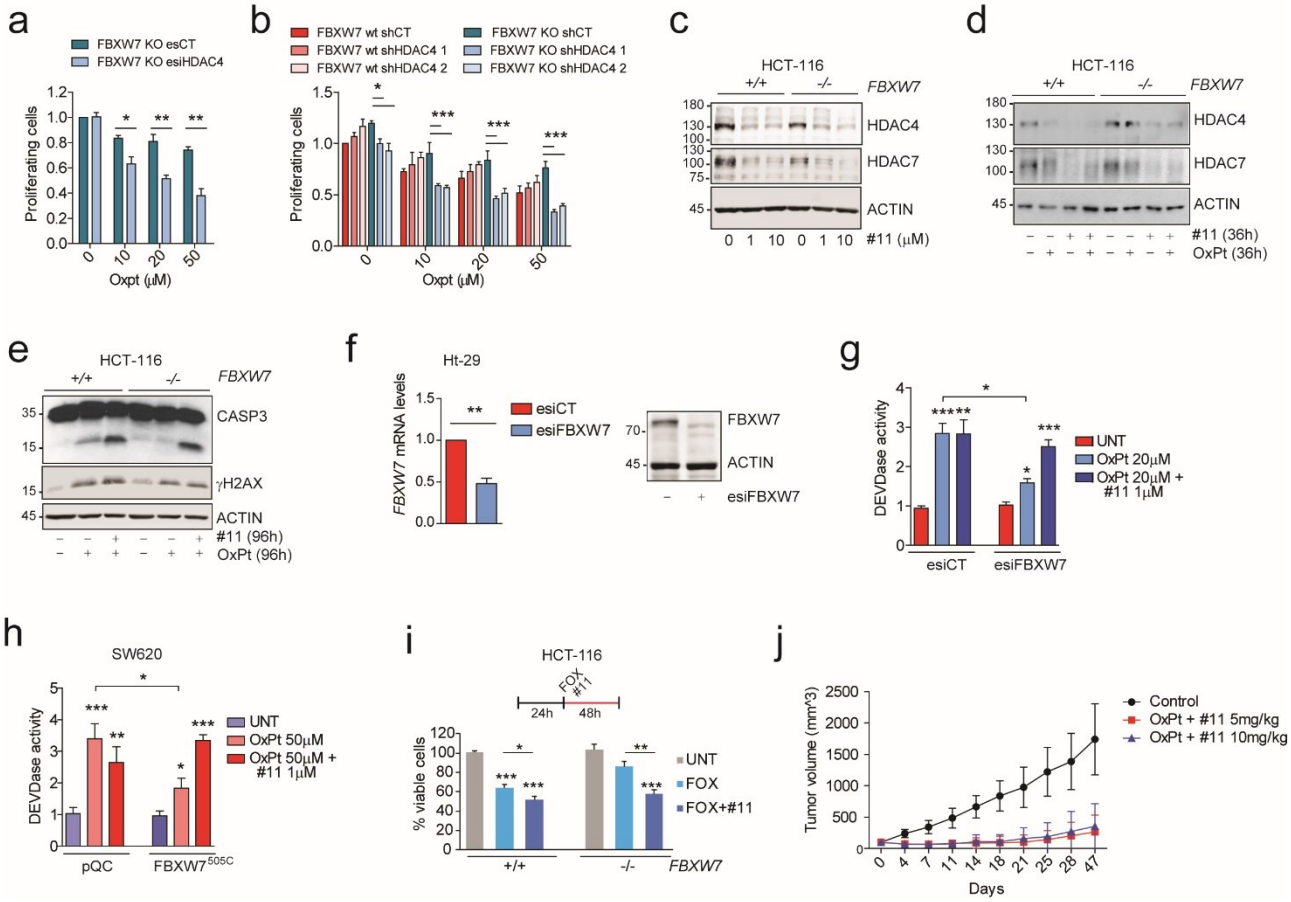

Supplementary Figure 4. HDAC4 forced degradation or silencing increased OxPt cytotoxicity. a. Fraction of proliferating HCT-116 *FBXW7*$^{-/-}$ cells silenced or not for HDAC4 for 24h and then treated with the indicated concentrations of OxPt for 72h, evaluated by resazurin assay. n=3 **b.** Fraction of proliferating HCT-116 cells WT or *FBXW7*$^{-/-}$ in which HDAC4 expression was stably knocked-down with the indicated shRNAs and treated with the indicated concentrations of OxPt for 72h, evaluated by resazurin assay. n=5. **c,d.** Immunoblot analysis of the indicated proteins in HCT-116 WT or *FBXW7*$^{-/-}$ cells treated as indicated for 36h (in d: OxPt 50μM, #11 1μM). **e**. Immunoblot analysis of the indicated proteins in HCT-116 WT or *FBXW7*$^{-/-}$ cells treated with OxPt 50μM and #11 1μM, as indicated. **f.** mRNA and protein levels of FBXW7 from Ht-29 cells transfected with esiCT and esiFBXW7 for 72h. **g.** DEVDase activity evaluated by Apo-ONE assay in Ht-29 cells silenced or not with esiFBXW7 for 72 h and treated with OxPt 10μM or OxPt 10μM + #11 1μM for the last 48. n=3. **h.** DEVDase activity evaluated by Apo-ONE assay in SW620 cells overexpressing or not FBXW7 R505C, treated with OxPt 50μM or OxPt 50μM + #11 1μM for 48h. n=3. **i.** Histogram showing the percentage of HCT-116 WT or *FBXW7*$^{-/-}$ viable cells after 72h of the indicated treatments (FOX: 5-FU 20μM + OxPt 20μM; #11 1μM), evaluated by resazurin assay. n=3. **j.** Tumour volumes of the HCT-116 *FBXW7*$^{-/-}$ xenograft model in mice treated twice per week with vehicle (n=9), OxPt 5 mg/kg + PROTAC #11 5 mg/kg (n=10), or OxPt 5 mg/kg + PROTAC #11 10 mg/kg (n=9), until day 47. In a, b, f, h, i, j data are reported as means ± st.dev. t-test for pairwise comparison, Dunn-multiple comparison test for multiple testing.

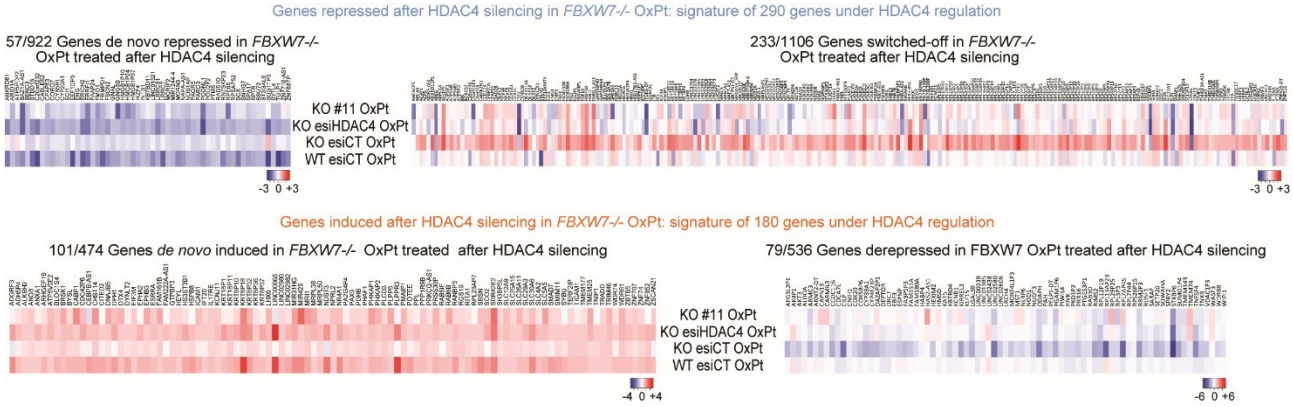

Supplementary Figure 5. Identification of a signature of genes that are differentially perturbed by OxPt in HCT-116 WT and *FBXW7*$^{-/-}$ cells, but whose transcriptional response in *FBXW7*$^{-/-}$ cells after silencing or forced degradation of HDAC4 is made similar to that of WT cells. Heatmaps showing the strong dependence on HDAC4 for the transcriptional control of the identified signatures.

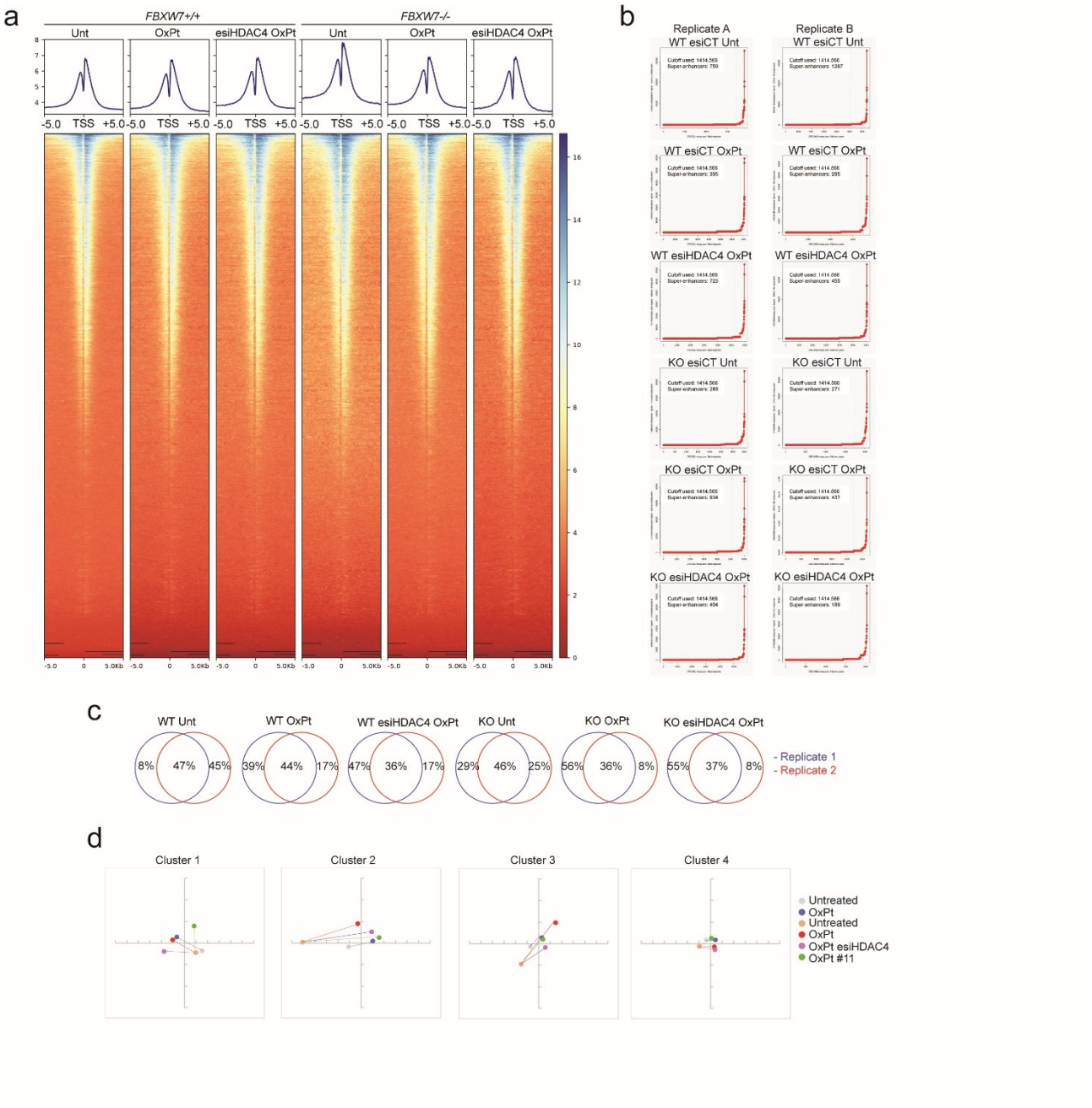

Supplementary Figure 6. OxPt treatment and HDAC4 depletion do not result in global alterations of the H3K27ac profile but in profound changes focused at the level of well-defined super-enhancers that are conserved between the two biological replicates. a. Heat-maps of H3K27ac levels distribution within 10kb around the transcription start site (TSS) in the indicated samples. **b.** H3K27ac ranking generated by ROSE algorithm identifying the indicated number of SEs in the different samples and treatment conditions. **c.** Venn diagrams displaying the percentage of overlap between the SEs identified in two biological replicates of each sample. **d.** PCA analysis of H3K27ac data within 40kb of the center of the SE belonging to each cluster, as indicated. The dotted line highlights the Euclidean distance between each untreated and OxPt-treated sample.

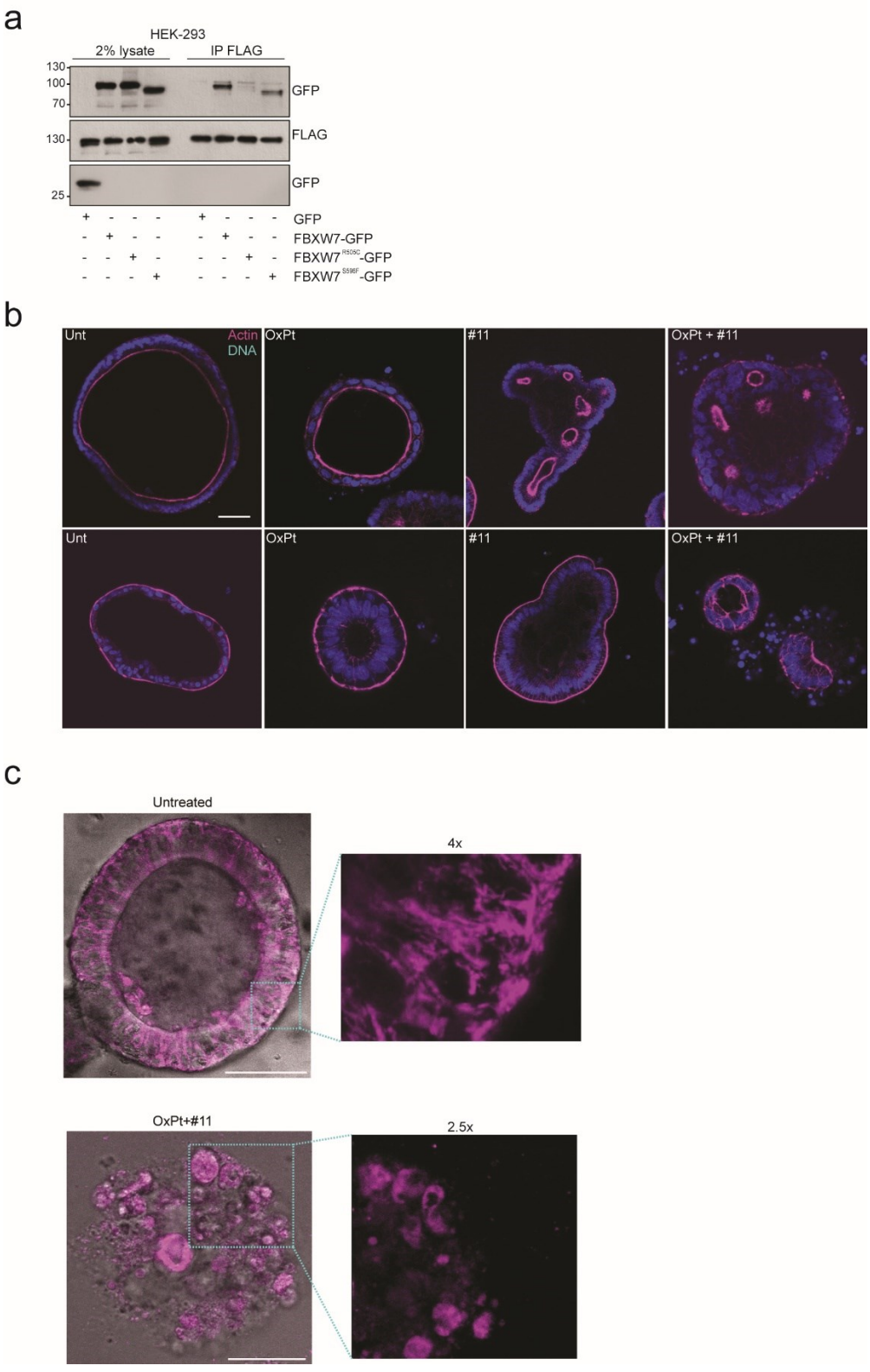

Supplementary Figure 7. Characterization of PDOs. a. 293 cells were transfected with GFP, GFP-FBXW7, GFP-FBXW7^{R505C} or GFP-FBXW7^{S596F} and HDAC4-FLAG and treated for 24h with 50μM OxPt and for the last 12h with 2.5μM MG132. FBXW7 and FBXW7^{S596F}, but not FBXW7^{505C}, were co-immunopurified by anti-FLAG. **b.** Representative confocal images of equatorial sections of PDM-96, treated as indicated and displaying normal polarity (above) or inverted polarity (TSIPs, quantified in Fig. 7b). Scale bar = 50 μm. **c.** PDM-96 PDOs, pre-treated for 96h with OxPt+#11 or left untreated, were loaded for 30' with TMRM and imaged by confocal live-imaging. Mitochondrial fragmentation and dissipation of Δψm was evident in OxPt+#11 co-treatment. Scale bar = 45 μm.

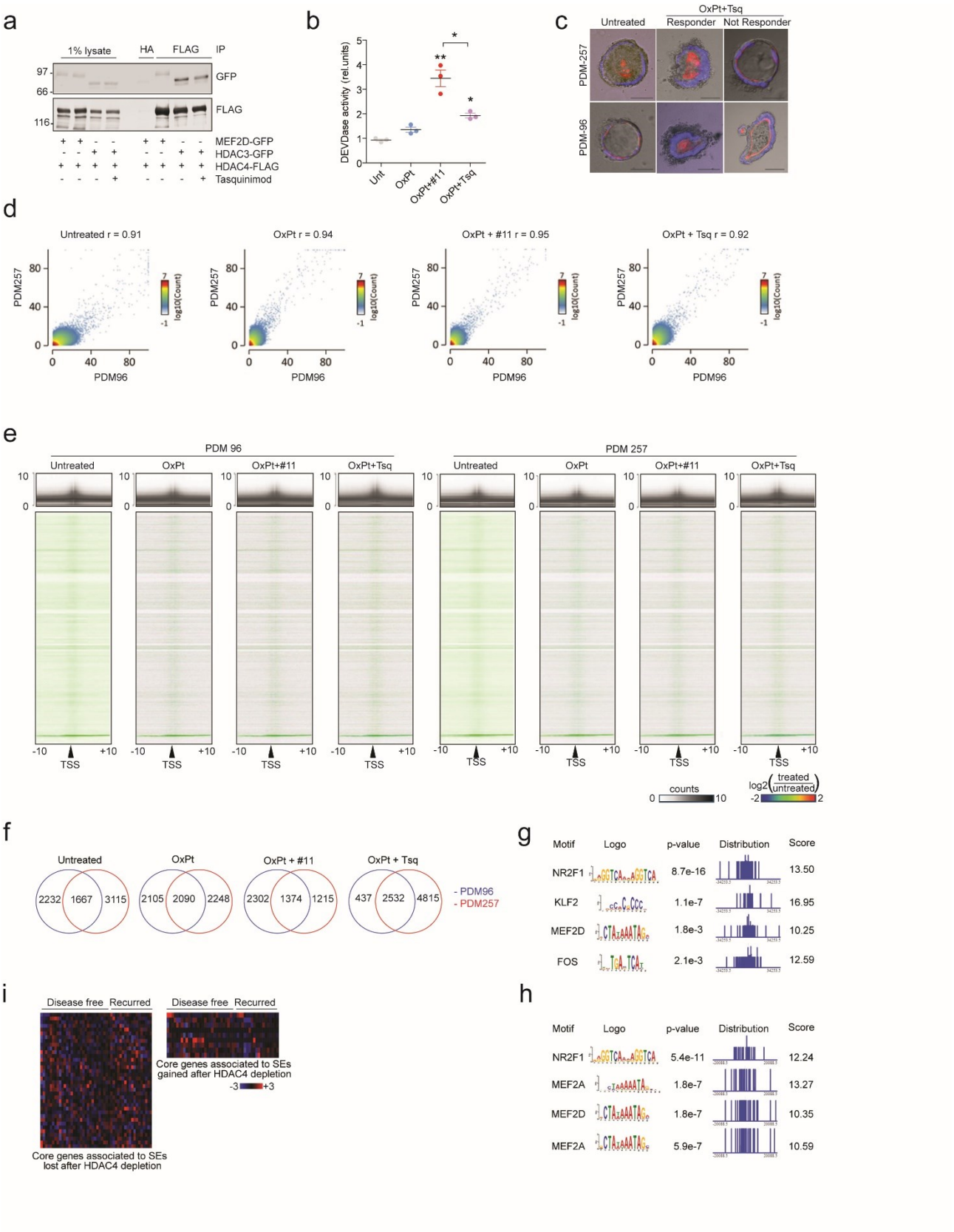

Supplementary Figure 8. Dissection of the epigenetic response correlating with sensitivity or resistance to Pt-based chemotherapy. a. 293 cells were transfected as indicated and treated or not for 24h with 1 µM OxPt, as indicated. Cells were harvested, lysed and subjected to immunoprecipitation with 1µg anti-FLAG or anti-HA (as a control) antibodies. **b.** DEVDase activity evaluated by Apo-ONE assay in PDM-96 treated with OxPt 50µM or OxPt 50µM + #11 1µM or OxPt 50µM + Tsq 1µM for 96h. n=3. **c.** Representative images of PDM-96 and PDM-257 displaying accumulation of apoptotic bodies (responders) or not (not responders) after

treatment with OxPt 50μM + Tsq 1μM for 96h. Overlay of brightfield and epifluorescence images is shown (Red=actin, Blue=DNA, Hoechst staining). Scale bar= 40 μm. **d.** Pearson correlation plot between H3K27ac signal and density between the indicated samples. **e.** Heat-maps showing H3K27ac levels and density relative to untreated condition, within 20kb from the TSS. **f.** Venn diagrams displaying the overlap between the SEs identified for each treatment condition in PDM-96 and PDM-257. **g,h.** Motif enrichment analysis (SEA) within "refined cluster 2" (g) or "refined cluster 3" of SEs, as defined in the manuscript. **i.** Heat-map of the expression levels (z-score) in 47 CRC patients from the Sidra-LUMC AC-ICAM cohort[71] of the minimal signatures of 37 and 9 genes identified and associated to refined cluster 2 and 3 of SEs. Expression levels of the identified signatures in biopsies from untreated samples successfully segregate a priori patients that will respond to Pt-based adjuvant chemotherapy from not-responder ones.

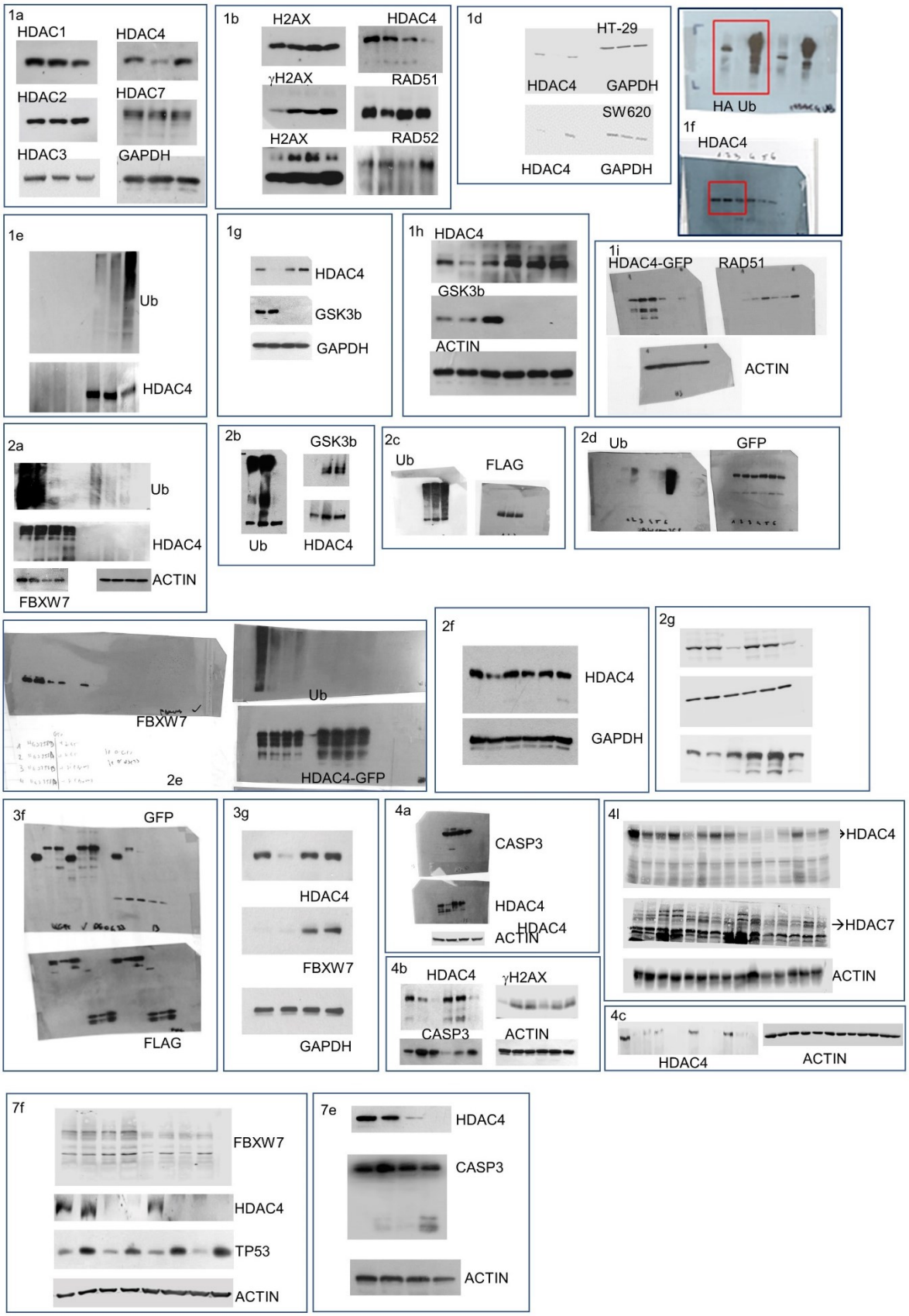

Supplementary Figure 9. Original images used for the composition of the immunoblot panels in the main figures.

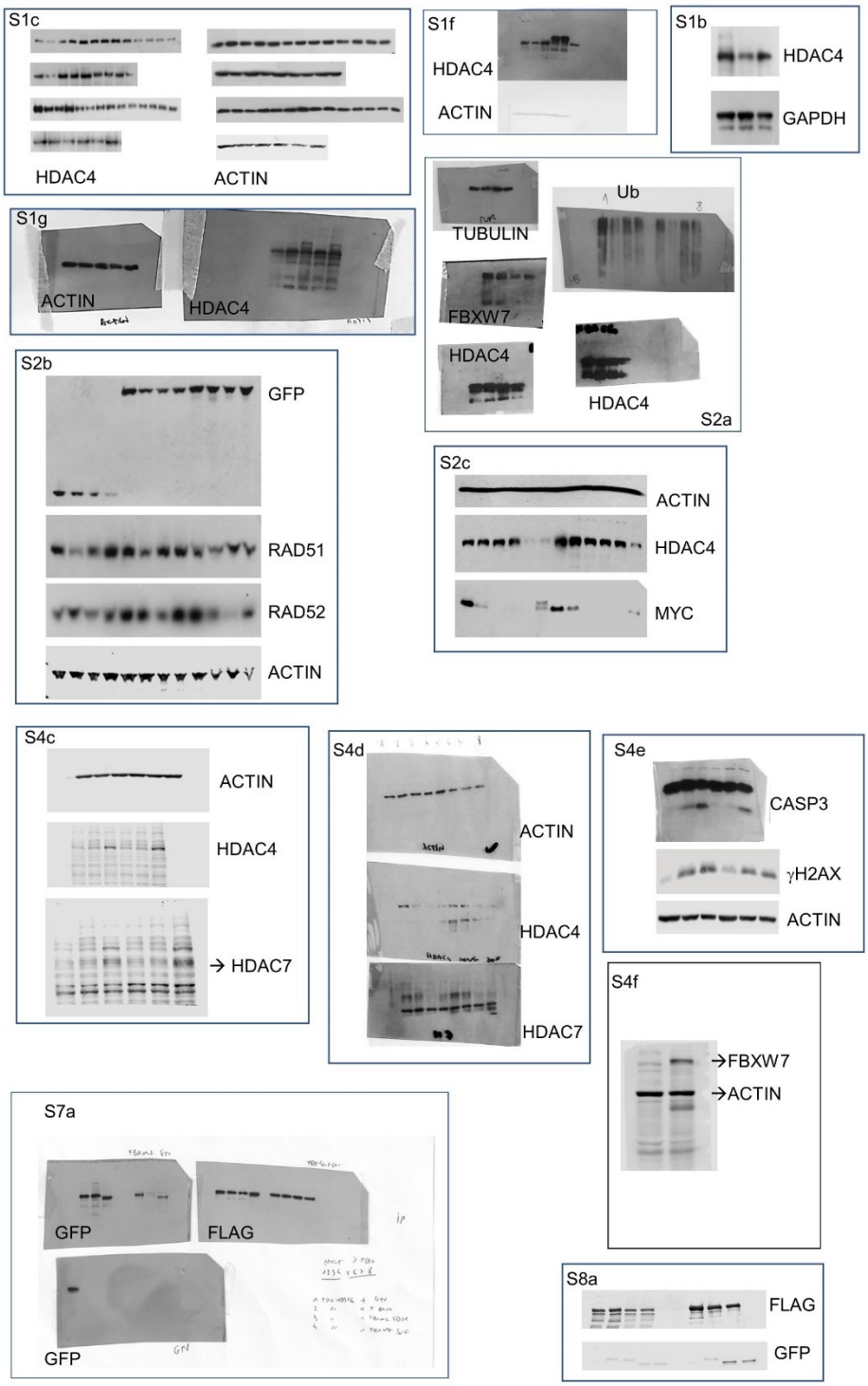

Supplementary Figure 10. Original images used for the composition of the immunoblot panels in the supplementary figures.